

Bonding and Stability of the Hydrogen Storage Material Mg₂NiH₄Ulrich Häussermann,^{*†} Helen Blomqvist,[‡] and Dag Noréus[‡]

Departments of Inorganic Chemistry and Structural Chemistry, Stockholm University, S-10691 Stockholm, Sweden

Received February 6, 2002

Structural stability and bonding properties of the hydrogen storage material Mg₂NiH₄ (monoclinic, *C2/c*, *Z* = 8) were investigated and compared to those of Ba₂PdH₄ (orthorhombic, *Pnma*, *Z* = 8) using ab initio density functional calculations. Both compounds belong to the family of complex transition metal hydrides. Their crystal structures contain discrete tetrahedral 18 electron complexes T⁰H₄⁴⁻ (T = Ni, Pd). However, the bonding situation in the two systems was found to be quite different. For Ba₂PdH₄, the electronic density of states mirrors perfectly the molecular states of the complex PdH₄⁴⁻, whereas for Mg₂NiH₄ a clear relation between molecular states of TH₄⁴⁻ and the density of states of the solid-state compound is missing. Differences in bonding of Ba₂PdH₄ and Mg₂NiH₄ originate in the different strength of the T–H interactions (Pd–H interactions are considerably stronger than Ni–H ones) and in the different strength of the interaction between the alkaline-earth metal component and H (Ba–H interactions are substantially weaker than Mg–H ones). To lower the hydrogen desorption temperature of Mg₂NiH₄, it is suggested to destabilize this compound by introducing defects in the counterion matrix surrounding the tetrahedral Ni⁰H₄⁴⁻ complexes. This might be achieved by substituting Mg for Al.

1. Introduction

The compound Mg₂NiH₄ attracts wide interest for being a promising hydrogen storage material and for its unusual structural and bonding properties.¹ Mg₂NiH₄ forms readily by hydrogenating the alloy Mg₂Ni.² However, an intricate temperature polymorphism is observed which comprises two different low-temperature forms (designated as LT1 and LT2 in the literature) and a high-temperature modification (HT).^{3,4} LT1 is obtained when hydrogenating Mg₂Ni at low temperatures (around 180 °C). Upon heating above 235 °C, LT1 transforms into HT which yields LT2 under cooling below the transition temperature. LT2 corresponds to a microtwinned variant of LT1.^{5,6} It is not yet clear if there are

genuine structural differences between LT1 and LT2.⁷ The unique monoclinic structure of low-temperature Mg₂NiH₄, as reported by Zolliker et al.,⁸ contains discrete tetrahedral Ni⁰H₄⁴⁻ complexes. In the cubic HT structure, the location of the H atoms is not fully established as these atoms perform some kind of reorientational motion around the central Ni atoms.⁹ Thus, the hydrogen positions are usually described as a random distribution over the positions of an octahedron around Ni.¹⁰ However, recent theoretical calculations point to a flattened tetrahedral coordination of Ni by H in HT-Mg₂NiH₄.¹¹

The occurrence of a low-valent hydrido complex Ni⁰H₄⁴⁻ in Mg₂NiH₄ is interesting because low oxidation states are usually associated with π-bonded, electron accepting ligands. This conventional stabilization by “back-donation” to ligand orbitals is, however, not available in homoleptic hydrido complexes. Ni⁰H₄⁴⁻ in Mg₂NiH₄ and CaMgNiH₄¹² represents the only known low-valent Ni hydrido complex. This is in contrast to the higher congener Pd. Apart from the tetrahedral

* To whom correspondence should be addressed. E-mail: ulrich@inorg.su.se.

† Department of Inorganic Chemistry.

‡ Department of Structural Chemistry.

- (1) Sandrock, G.; Suda, S.; Schlapbach, L. *Topics in Applied Physics, Hydrogen in Intermetallic Compounds*; Springer: Berlin, 1992; Vol. 67, p 210. Dantzer, P. *Topics in Applied Physics, Hydrogen in Metals III*; Springer: Berlin, 1997; Vol. 73, p 279.
- (2) Reilly, J. J.; Wishall, R. H., Jr. *Inorg. Chem.* **1968**, *7*, 2254.
- (3) Gavra, Z.; Kimmel, G.; Gefen, Y.; Mintz, M. H. *J. Appl. Phys.* **1985**, *57*, 4548.
- (4) Ono, S.; Hayakawa, H.; Suzuki, A.; Nomura, K.; Nishimiya, N.; Tabata, T. *J. Less-Common Met.* **1982**, *88*, 63.
- (5) Zolliker, P.; Yvon, K.; Baerlocher, C. *J. Less-Common Met.* **1986**, *115*, 65.
- (6) Noréus, D.; Kihlberg, L. *J. Less-Common Met.* **1986**, *123*, 233.

- (7) Blomqvist, H.; Noréus, D. *J. Appl. Phys.* **2002**, *91*, 5141.
- (8) Zolliker, P.; Yvon, K.; Jorgensen, J. D.; Rotella, F. J. *Inorg. Chem.* **1986**, *25*, 3590.
- (9) Noréus, D.; Olsson, L. G. *J. Chem. Phys.* **1983**, *78*, 2419.
- (10) Gavra, Z.; Mintz, M. H.; Kimmel, G.; Hadari, Z. *Inorg. Chem.* **1979**, *18*, 3595.
- (11) García, G. N.; Abriata, J. P.; Sofu, J. O. *Phys. Rev. B* **1999**, *59*, 11746.
- (12) Huang, B.; Yvon, K.; Fischer, P. *J. J. Alloys Compd.* **1992**, *178*, 173.

$Pd^0H_4^{4-}$ complexes in Sr_2PdH_4 , Ba_2PdH_4 ,¹³ and Eu_2PdH_4 ,¹⁴ additionally, linear $Pd^0H_2^{2-}$ in Li_2PdH_2 and Na_2PdH_2 ¹⁵ and a trigonal planar $Pd^0H_3^{3-}$ in $NaBaPdH_3$ ¹⁶ were found. Concerning the compounds A_2PdH_4 ($A = Sr, Ba, Eu$), their structure type corresponds to orthorhombic β - K_2SO_4 which is widely adopted among compounds with tetrahedral complex anions.

In this work, we aim to elucidate the electronic structure of Mg_2NiH_4 in its monoclinic LT structure and relate it to that of Ba_2PdH_4 with the β - K_2SO_4 structure. In particular, we try to find the nature of the stabilizing mechanism of the electron dense tetrahedral hydrido complexes in these compounds. Second, we try to establish some general differences between Ni and Pd hydrido complex compounds (i.e., why do Pd complexes seem to be more abundant than Ni ones?). Importantly, we consider a detailed knowledge of the electronic structure of Mg_2NiH_4 as invaluable for applied research. Because the hydrogen desorption temperature is somewhat too high for convenient storage applications, intense research is focused presently on possibilities to lower the thermal stability of Mg_2NiH_4 .¹⁷ Mg_2NiH_4 has already been the subject of several theoretical investigations.^{11,18–20} However, none of them considered the quite complex monoclinic LT structure, but rather, they focused on the simpler HT form applying different structural models for describing hydrogen disorder.

2. Computational Section

Total energy calculations for the ternary systems Mg_2NiH_4 , Ba_2PdH_4 , Ba_2NiH_4 , and Mg_2PdH_4 (Ae_2TH_4) and the binary compounds MgH_2 and BaH_2 (AeH_2) were performed within ab initio density functional theory using pseudopotentials and a plane wave basis set as implemented in the program VASP.²¹ Concerning the pseudopotentials, ultrasoft Vanderbilt-type pseudopotentials²² were employed considering nd and $(n + 1)s$ electrons as valence electrons for Ni and Pd, $3s$ electrons for Mg, and $5p$ and $6s$ electrons for Ba. For Ae_2TH_4 , the atomic position parameters and lattice parameters of the structure types Mg_2NiH_4 (monoclinic) and β - K_2SO_4 (orthorhombic) were relaxed for a set of constant volumes until forces had converged to less than 0.01 eV/\AA . In a second step, we extracted the equilibrium volume V_0 and the ground-state energy E_0 by fitting the E versus V values to a Birch–Murnaghan equation of state. For AeH_2 , the same procedure was applied to rutile MgH_2 ²³ and

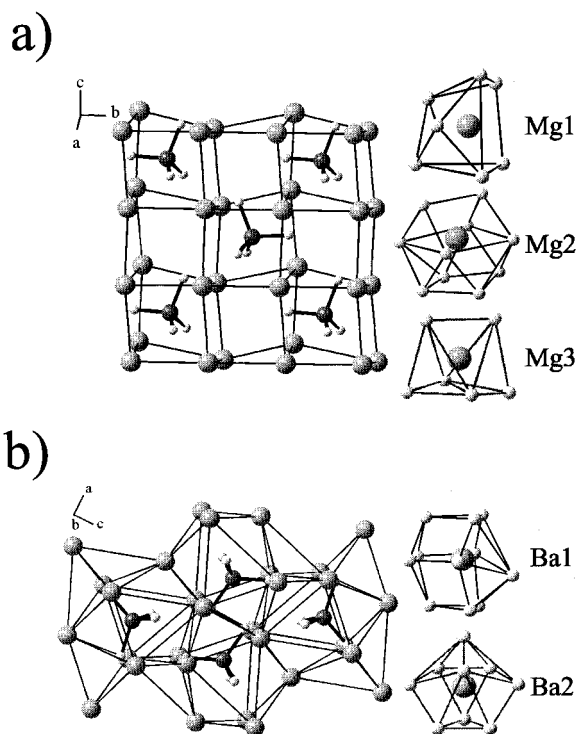


Figure 1. Crystal structures of monoclinic Mg_2NiH_4 (a) and orthorhombic Ba_2PdH_4 (b) together with the H coordination polyhedra of the alkaline-earth metals.

$BaCl_2$ -type BaH_2 .²⁴ The exchange and correlation energy was assessed by the generalized gradient approximation (GGA).²⁵ Convergence of the calculations was carefully checked with respect to the plane wave cutoff and the number of k points used in the summation over the Brillouin zone. Concerning the plane wave cutoff, an energy value of 500 eV was chosen for all systems. This high value was found to be necessary to achieve complete convergence with respect to the basis set. The k points were generated by the Monkhorst–Pack method²⁶ and sampled on grids of $4 \times 4 \times 4$ (Ae_2TH_4), $8 \times 8 \times 8$ (MgH_2), and $6 \times 6 \times 6$ (BaH_2). The integration over the Brillouin zone was performed by the improved tetrahedron method.²⁷

3. Results and Discussion

3.1. Structural Stability and Physical Properties. The structures of monoclinic Mg_2NiH_4 (space group $C2/c$, $Z = 8$)⁸ and orthorhombic Ba_2PdH_4 (space group $Pnma$, $Z = 8$)¹³ are depicted in Figure 1a,b, respectively. In Mg_2NiH_4 , tetrahedral $Ni^0H_4^{4-}$ complexes are embedded in a distorted simple cubic arrangement of Mg^{2+} counterions. The metal atoms Mg and Ni together form a distorted antifluorite structure which provides H with an approximate tetrahedral coordination (1 Ni and 3 Mg). The MgH_n coordination polyhedra are rather irregular with $n = 7$ for Mg1 (distorted monocapped trigonal prism), $n = 6 + 4$ for Mg2 (trigonal

(13) Olofsson-Mårtensson, M.; Kritikos, M.; Noréus, D. *J. Am. Chem. Soc.* **1999**, *121*, 10908.

(14) Kohlmann, H.; Fischer, H. E.; Yvon, K. *Inorg. Chem.* **2001**, *40*, 2608.

(15) Kadir, K.; Noréus, D. *Z. Phys. Chem. (Muenchen)* **1989**, *163*, 231. Noréus, D.; Törnroos, K. W.; Börje, A.; Szabó, T.; Bronger, W.; Spittank, H.; Auffermann, G.; Müller, P. *J. Less-Common Met.* **1988**, *139*, 233.

(16) Olofsson, M.; Kritikos, M.; Noréus, D. *Inorg. Chem.* **1998**, *37*, 2900.

(17) Blomqvist, H.; Rönnebro, E.; Noréus, D.; Kuji, T. *J. Alloys Compd.* **2002**, *330–332*, 268. Guthrie, S. E.; Thomas, G. J.; Noréus, D.; Rönnebro, E. *Mater. Res. Soc. Symp. Proc.* **1998**, *513*, 93.

(18) Gupta, M. *J. Less-Common Met.* **1984**, *101*, 35.

(19) Gupta, M.; Belin, E.; Schlapbach, L. *J. Less-Common Met.* **1984**, *103*, 389.

(20) Takahashi, Y.; Yukawa, H.; Morinaga, M. *J. Alloys Compd.* **1996**, *242*, 98.

(21) Kresse, G.; Hafner, J. *Phys. Rev. B* **1993**, *47*, RC558. Kresse, G.; Furthmüller, J. *Phys. Rev. B* **1996**, *54*, 11169.

(22) Vanderbilt, D. *Phys. Rev. B* **1990**, *41*, 7892. Kresse, G.; Hafner, J. *J. Phys.: Condens. Matter* **1994**, *6*, 8245.

(23) Zachariasen, W. H.; Holley, C. E., Jr.; Stamper, J. F., Jr. *Acta Crystallogr.* **1963**, *16*, 352.

(24) Bronger, W.; Chi Chien, S.; Müller, P. *Z. Anorg. Allg. Chem.* **1987**, *545*, 69.

(25) Perdew, J.; Wang, Y. *Phys. Rev. B* **1992**, *45*, 13244.

(26) Monkhorst, H. J.; Pack, J. D. *Phys. Rev. B* **1976**, *13*, 5188.

(27) Blöchl, P.; Jepsen, O.; Andersen, O. K. *Phys. Rev. B* **1994**, *49*, 16223.

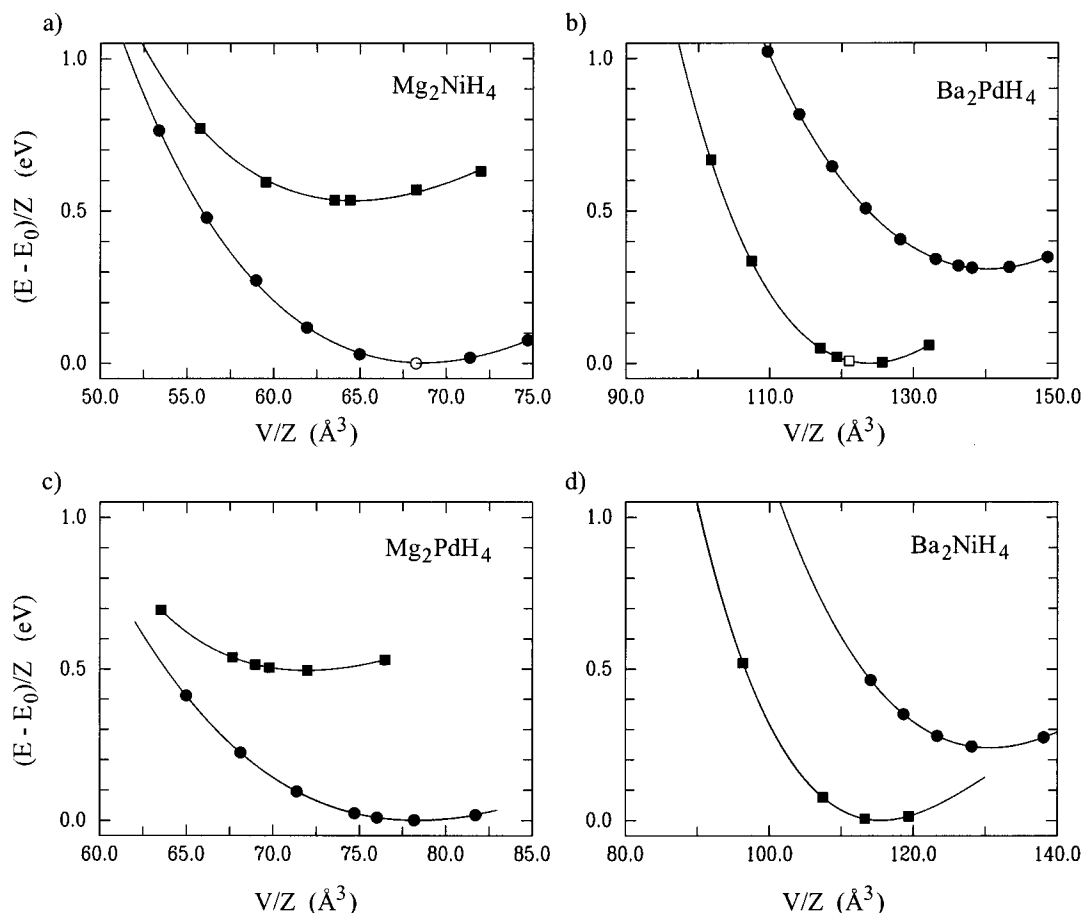


Figure 2. Structural competition between the monoclinic Mg_2NiH_4 structure (●) and the orthorhombic $\beta\text{-K}_2\text{SO}_4$ structure (■) in the systems Mg_2NiH_4 (a), Ba_2PdH_4 (b), Mg_2PdH_4 (c), and Ba_2NiH_4 (d). E_0 is the energy of the calculated ground-state equilibrium volume. Open symbols denote experimental equilibrium volumes.

prism with an attached square, the latter ligands are considerably farther away from Mg_2 , and $n = 6$ for Mg_3 (monocapped trigonal bipyramid). In Ba_2PdH_4 , the arrangement of the Ba^{2+} ions around the tetrahedral $\text{Pd}^0\text{H}_4^{4-}$ complexes may be described as a distorted tricapped trigonal prism. H is surrounded by six metal atoms (1 Pd and 5 Ba) in an octahedral fashion. The H coordination numbers of Ba are 11 and 9 for Ba1 and Ba2, respectively.

We started our investigation by comparing the structural stability of Mg_2NiH_4 and Ba_2PdH_4 as well as that of hypothetical Mg_2PdH_4 and Ba_2NiH_4 in the Mg_2NiH_4 and the $\beta\text{-K}_2\text{SO}_4$ structure. The latter systems were considered in order to extract the influence of the alkaline-earth metal (Ae) component on structural stability. The results are shown in Figure 2. The ground-state structures of Mg_2NiH_4 and Ba_2PdH_4 are reproduced correctly by theory and are well separated by 0.54 and 0.31 eV/Z, respectively, from the respective structural alternative (Figure 2a,b). In both systems, the $\beta\text{-K}_2\text{SO}_4$ structure type attains a lower equilibrium volume compared to the Mg_2NiH_4 structure. This fact is not surprising because the higher coordination numbers of Ae and H in the $\beta\text{-K}_2\text{SO}_4$ type realize a more densely packed structure. The size and, thus, the coordination of the Ae component have a decisive role in determining the structure type. This is seen in the hypothetical systems Mg_2PdH_4 and Ba_2NiH_4 for which the Mg_2NiH_4 and the $\beta\text{-K}_2\text{SO}_4$

Table 1. Lattice Parameters for Mg_2NiH_4 and Ba_2PdH_4 ^a

	Mg_2NiH_4 monoclinic	Ba_2PdH_4 orthorhombic
V/Z [\AA^3]	68.44 68.25	123.64 117.47
a [\AA]	14.3727 <i>14.343</i>	8.1808 <i>8.0081</i>
b [\AA]	6.3963 <i>6.4038</i>	5.8432 <i>5.7688</i>
c [\AA]	6.4864 <i>6.4830</i>	10.3459 <i>10.171</i>
β [deg]	113.34 <i>113.52</i>	

^a Experimental values are given in italics.

structure, respectively, are most stable (Figure 2c,d). Thus, systems containing the small Mg^{2+} ions prefer a structure type which provides smaller H coordination numbers for the Ae component (and smaller Ae–H distances), and vice versa, for systems with the large Ba^{2+} ions, a structure type is adopted which enables larger H coordination numbers. If we compare the experimental structural parameters with the computationally modeled ones (Tables 1 and 2), we observe a close agreement for Mg_2NiH_4 concerning the lattice parameters as well as the atomic position parameters. For Ba_2PdH_4 , the theoretical ground state volume is overestimated by more than 5% leading to deviations between calculated and experimental lattice parameters of

Table 2. Atomic Position Parameters for Mg₂NiH₄ and Ba₂PdH₄^a

Mg ₂ NiH ₄				
	C2/c	x	y	z
Mg1	8f	0.2645	0.4872	0.0829
		0.2652	0.4827	0.0754
Mg2	4e	0	0.0262	0.25
		0	0.0244	0.25
Mg3	4e	0	0.5272	0.25
		0	0.5130	0.25
Ni	8f	0.1201	0.2298	0.0800
		0.1194	0.2308	0.0832
H1	8f	0.2092	0.3045	0.3043
		0.2113	0.2995	0.3037
H2	8f	0.1390	0.3207	0.8760
		0.1360	0.3163	0.8811
H3	8f	0.0105	0.2918	0.0552
		0.0105	0.2868	0.0537
H4	8f	0.1244	0.9868	0.0716
		0.1306	0.9950	0.0815
Ba ₂ PdH ₄				
	Pnma	x	y	z
Ba1	4c	0.8528	0.25	0.5947
		0.8531	0.25	0.5973
Ba2	4c	0.0109	0.25	0.1680
		0.0128	0.25	0.1678
Pd	4c	0.2582	0.25	0.5829
		0.2598	0.25	0.5808
H1	4c	0.1748	0.25	0.4206
		0.174	0.25	0.420
H2	4c	0.4758	0.25	0.6077
		0.484	0.25	0.608
H3	8d	0.1793	0.9947	0.6554
		0.1779	0.993	0.6599

^a Experimental values are given in italics.**Table 3.** Calculated Bulk Moduli (*B*₀) and Band Gaps (*E*_g) of the Investigated Hydrides

	<i>B</i> ₀ [GPa]	<i>E</i> _g [eV]
Mg ₂ NiH ₄	50.0	1.54
Ba ₂ PdH ₄	38.2	1.53
Mg ₂ PdH ₄	35.5	1.72
Ba ₂ NiH ₄	37.2	1.10
MgH ₂	48.0	3.78
BaH ₂	30.3	2.79

around 2%. The overestimation of ground state volumes is frequently observed when using GGA for assessing exchange and correlation energy. However, the axis ratios and atomic position parameters are well reproduced.

We now turn to the discussion of some selected ground-state properties of the investigated systems (cf. Table 3). Mg₂NiH₄ and Ba₂PdH₄ are semiconductors with calculated band gaps of 1.54 and 1.53 eV, respectively. The band gap of Mg₂NiH₄ has been determined experimentally. The value of the LT form is 1.68 eV,²⁸ which is in close agreement with our calculations. A similar size of the band gaps of Mg₂NiH₄ and Ba₂PdH₄ is indicated in the similar color of these compounds, which are reported to be brownish-grey²⁹ and dark brown,¹³ respectively. The hypothetical systems Mg₂PdH₄ (Mg₂NiH₄ structure) and Ba₂NiH₄ (β-K₂SO₄ structure) have band gaps of 1.72 and 1.1 eV, respectively. For comparison, the band gaps of the ionic, saltlike hydrides MgH₂ and BaH₂ are about twice as large as that of the ternary

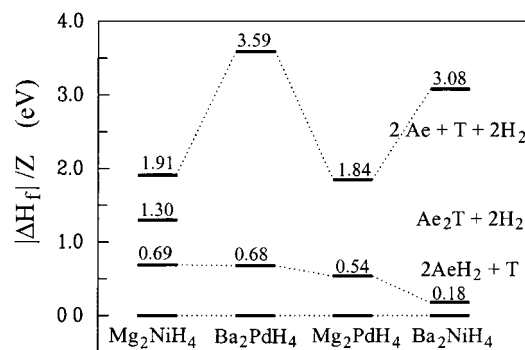
(28) Lupu, D.; Sârbu, R.; Biris, A. *Int. J. Hydrogen Energy* **1987**, *12*, 425.(29) Noréus, D. *Z. Phys. Chem. (Muenchen)* **1989**, *163*, 575.

Figure 3. Calculated enthalpies of formation for the systems Ae₂TH₄. The particular enthalpies are defined as $\Delta E = E(\text{Ae}_2\text{TH}_4) - 2 \times E(\text{Ae}) - E(\text{T}) - 2 \times E(\text{H}_2)$; $\Delta E = E(\text{Ae}_2\text{TH}_4) - 2 \times E(\text{AeH}_2) - E(\text{T})$; $\Delta E = E(\text{Ae}_2\text{TH}_4) - E(\text{Ae}_2\text{T}) - 2 \times E(\text{H}_2)$ and were extracted from calculations of the lowest energy of the respective Ae, AeH₂, Ae₂T, and T ground-state structures as well as the energy of a H₂ dimer. The magnetic structure of Ni (ferromagnetic) was considered.

transition metal hydrides. Further, we calculated the bulk moduli of the ternary and binary hydrides. The bulk modulus *B* is inverse to the compressibility of a material and parallels its hardness. Among the four transition metal hydrides, Mg₂NiH₄ has the highest bulk modulus (50 GPa), which interestingly is about the same as that of binary MgH₂. The other ternary compounds have similar *B* values of slightly below 40 GPa. Finally, we computed enthalpies of formation (i.e., at zero temperature) for the four transition metal hydrides. Apart from the formation from the elements, we also considered the more interesting formation from the hydrides and, in the case of Mg₂NiH₄, also the formation from the alloy Mg₂Ni. For the other systems, alloys with the Ae₂T composition are not known. The results are compiled in Figure 3. Mg₂NiH₄ and Ba₂PdH₄ are, by 0.69 and 0.68 eV/Z, respectively, more stable than 2AeH₂ + T. For hypothetical Mg₂PdH₄, the corresponding value is just slightly lower (0.54 eV/Z), which indicates that it might actually be possible to synthesize Mg₂PdH₄ from this reaction. Mg₂NiH₄ is by 1.30 eV/Z more stable than Mg₂Ni + 2H₂, the conventional hydrogenation reaction. This calculated value is in very good agreement with the experimental desorption enthalpy of 1.33 eV/Z (64 kJ/mol H₂).² In conclusion, the applied theoretical method is able to reproduce structural stability, structural parameters, and physical properties of LT-Mg₂NiH₄ and Ba₂PdH₄ in a highly satisfactory manner. In the next step, we analyze the electronic structure and chemical bonding of these compounds.

3.2. Chemical Bonding. TH₄⁴⁻. The natural starting point for a chemical bonding analysis of compounds Ae₂TH₄ is to look at the bonding in an isolated tetrahedral complex entity. A qualitative MO diagram is easily established and shown in Figure 4. When assuming T *nd* and (*n* + 1)*s* states as bonding active (sd^{*n*} hybridized transition metals), the resulting 10 MOs are divided into four bonding (*a*₁ and *t*₂), two nonbonding (*e*), and four antibonding ones (2*a*₁ and 2*t*₂; Figure 4a). With the inclusion of T (*n* + 1)*p* orbitals as basis functions (Figure 4b), an additional set of *t*₂ MOs can be constructed yielding a total of 4 bonding, 5 nonbonding, and

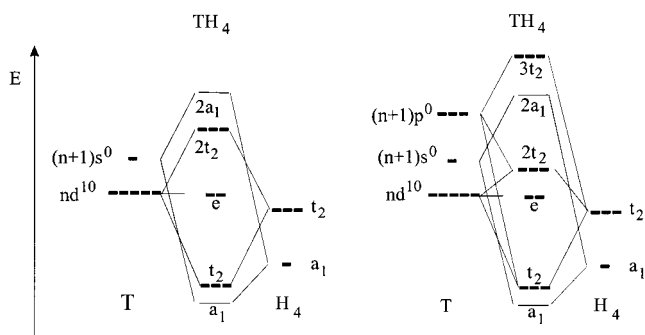


Figure 4. Approximate MO diagrams for a tetrahedral transition metal hydrido complex TH_4 . The diagram to the left-hand side is assembled from T-d and T-s atomic orbitals; that to the right-hand side includes T-p orbitals as well.

4 antibonding MOs. The two MO diagrams reflect two recently proposed bonding pictures for transition metal hydrido complexes. According to Firman and Landis,³⁰ the transition metal central atom is sd^n hybridized, whereas Bayse and Hall³¹ claim the necessity of the inclusion of T ($n + 1$)p orbitals for a correct bonding description. In particular, for tetrahedral 18 electron complexes TH_4^{4-} , the Firman–Landis model leads to a weakly bonded species because the antibonding $2t_2$ states have to be occupied and just one bonding MO (a_1) accounts for the complete ligand bonding (formal bond order T–H of 0.25). In the Bayse–Hall model, only bonding and nonbonding states are occupied, and ligand bonding can be described in terms of localized two-electron two-center T–H bonds. This, of course, provides a considerable admixture of T-p orbitals to the molecular states.

Ba_2PdH_4 . The density of states (DOS) of Ba_2PdH_4 (Figure 5a) mirrors very well the MO diagram depicted in Figure 4 in the energy region below the Fermi level. The bonding a_1 and t_2 based bands lowest in energy are merged, whereas the e and $2t_2$ states in the higher lying non/antibonding region are clearly resolved. Bands with a high contribution of H states (a_1 , t_2 , and $2t_2$) have a larger dispersion. This dispersion of bands based on molecular states is a consequence of the solid state: it originates basically from intertetrahedral H–H (closed-shell) interactions and to a minor degree from interactions of (empty) Ba^{2+} states with occupied PdH_4^{4-} states. The relative ratio of the integrated H and Pd-d states in the bonding ($a_1 + t_2$) and non/antibonding ($e + 2t_2$) part of the DOS (Table 4) gives some idea about the strength of the Pd–H orbital interactions.³² The d state distribution over these two parts is 26%/74%, and the one of the H states is 74%/26%. This points to rather strong Pd–H orbital interactions, especially, as we will see later on, in comparison with Ni–H interactions. The partial DOS of Pd (Figure 5a), which further is split into its orbital contributions, reveals that the admixture of Pd-p states into the occupied bands is negligible. Thus, we prefer to describe bonding of the tetrahedral 18

electron complex $\text{Pd}^0\text{H}_4^{4-}$ according to the Firman–Landis model³⁰ with just bonding active Pd d and s orbitals. The weakly bonded hydrido complex, which results from this bonding picture, experiences stabilization from the counterion matrix in the solid-state compound Ba_2PdH_4 . The admixture of empty Ba^{2+} states into the occupied PdH_4^{4-} ones (Figure 5a) releases partly antibonding states above the Fermi level. The validity of the Firman–Landis model to Pd-d¹⁰ hydrido complexes in general was especially established in our previous work where we compared distances and force constants of the Pd–H bonds in complexes with linear, trigonal planar, and tetrahedral geometry.³³ We observed a decreasing bond strength with increasing number of ligands, in line with the decreasing bond orders of 0.5, $1/3$, and 0.25, respectively, as obtained from the Firman–Landis model.

Mg_2NiH_4 . The DOS of Mg_2NiH_4 as shown in Figure 5b is remarkably different from that of Ba_2PdH_4 .³⁴ Most conspicuously, the clear relationship to the TH_4^{4-} MO diagram is lost. This is especially noticed in the large dispersion of the bonding a_1 and t_2 based bands (more than 5 eV). Additionally, the e and $2t_2$ based bands are merged. As for Pd, the orbital contributions of the partial DOS of Ni suggest that Ni-p states play a minor role in ligand bonding. The ratio of the Ni-d states in the bonding and non/antibonding region of the band structure (Table 4) is 15%/85%, and that of the H states, 79%/21%. These are considerably lower values compared to Ba_2PdH_4 and clearly indicate that Ni-d states are to a much lesser extent involved in H ligand bonding than Pd-d ones (i.e., the Ni–H orbital interactions are weaker than the Pd–H ones). The large dispersion of bands with a high H contribution (especially the low lying a_1 and t_2 , but also those bands based on $2t_2$) is due to the very short intertetrahedral H–H distances in Mg_2NiH_4 compared to Ba_2PdH_4 . In Table 5, selected distances in those compounds are listed. Whereas in Ba_2PdH_4 intertetrahedral H–H distances are generally larger than the intratetrahedral ones (2.84–3.04 Å), in Mg_2NiH_4 , intertetrahedral H–H distances can become as short as 2.44 Å and are not separated from the intratetrahedral ones (2.51–2.55 Å). Importantly, apart from the weaker T–H interactions in Mg_2NiH_4 , a second difference between Mg_2NiH_4 and Ba_2PdH_4 should be stronger interactions between the Ae component and the tetrahedral complex (or rather the H^- ligands) in the former because Mg^{2+} is a small and polarizing cation.

In the last step of our bonding analysis, we have to distinguish more unambiguously the influence of the transition metal component and the alkaline-earth metal counterions on the electronic structure. For this purpose, the

(30) Firman, T. K.; Landis, C. R. *J. Am. Chem. Soc.* **1998**, *120*, 12650.

(31) Bayse, C. A.; Hall, M. B. *J. Am. Chem. Soc.* **1999**, *121*, 1348.

(32) It is possible to calculate site projected densities of states from a plane wave basis set when defining spheres around the atomic sites. The obtained partial DOSs are dependent on the chosen radii of the spheres. However, the relative ratio of the integrated partial DOS in different, energetically resolved, parts of the DOS is almost insensitive to the chosen radii.

(33) Olofsson-Mårtensson, M.; Häussermann, U.; Tomkinson, J.; Noréus, D. *J. Am. Chem. Soc.* **2000**, *122*, 6960.

(34) The shape of the DOS of $\text{LT-Mg}_2\text{NiH}_4$ calculated by us is very similar to that of $\text{HT-Mg}_2\text{NiH}_4$ as obtained recently by García et al.¹¹ This is not surprising because the structural model of $\text{HT-Mg}_2\text{NiH}_4$ applied by García et al. was based on a regular antiferro arrangement of metal atoms in which Ni atoms were coordinated by four H atoms. The authors investigated the electronic structure influence of a flattening of $\text{Ni}^0\text{H}_4^{4-}$ tetrahedra towards a square planar arrangement. Thus, their structural model of $\text{HT-Mg}_2\text{NiH}_4$ is quite similar to the $\text{LT-Mg}_2\text{NiH}_4$ structure.

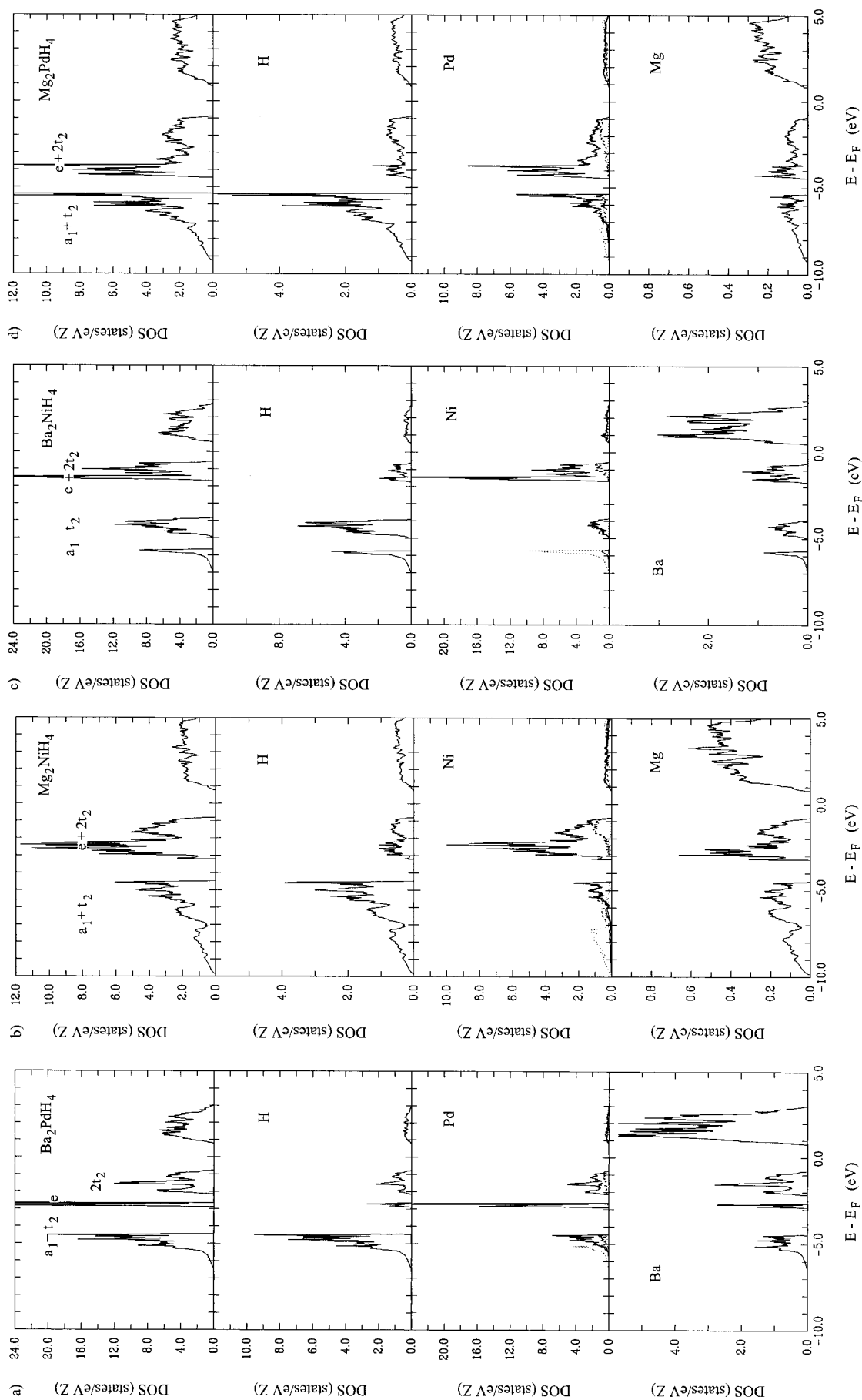


Figure 5. Total density of states (DOS) and partial DOS³² of the sites H, T, and Ae of the systems Mg_2NiH_4 (a), Ba_2PdH_4 (b), Ba_2NiH_4 (c), and Mg_2PdH_4 (d) calculated at the theoretical equilibrium volume of the respective lowest energy structure. Note that concerning the partial DOS of T also the decomposition into the orbital contributions d, s (.....), and p (---) is shown. The latter two contributions are scaled by a factor of 10. The T and T-d partial DOSs are basically indistinguishable in the figure. The Fermi level, E_F , is set to zero.

Table 4. Relative Ratio of T-d and H States (in percent) in the Bonding ($a_1 + t_2$) and Non/Antibonding ($e + 2t_2$) Parts of the DOS in the Systems Ae_2TH_4 ³²

	Ba_2PdH_4		Mg_2NiH_4		Ba_2NiH_4		Mg_2PdH_4	
	$a_1 + t_2$	$e + 2t_2$	$a_1 + t_2$	$e + 2t_2$	$a_1 + t_2$	$e + 2t_2$	$a_1 + t_2$	$e + 2t_2$
T-d	26	74	15	85	13	87	27	73
H	76	24	79	21	85	15	71	29

Table 5. Selected Distances [Å] in the Systems Ae_2TH_4 ^a

	Mg_2NiH_4	Mg_2PdH_4	Ba_2PdH_4	Ba_2NiH_4
	T–H			
	1.56 (1.52)	1.70	1.79 (1.81) × 2	1.64
	1.56 (1.52)	1.72	1.80 (1.81)	1.64 × 2
	1.57 (1.54)	1.75	1.81 (1.77)	1.64
	1.58 (1.57)	1.76		
	H–H _{intra}			
	2.52 (2.50)	2.74	2.85 (2.85) × 2	2.62 × 2
	2.53 (2.43)	2.75	2.89 (2.91) × 2	2.62 × 2
	2.53 (2.45)	2.78	2.98 (2.96)	2.70
	2.55 (2.47)	2.81	3.13 (3.13)	2.88
	2.55 (2.51)	2.81		
	2.67 (2.68)	2.92		
	H–H _{inter}			
	2.44 (2.42)	2.44	2.86 (2.80)	2.99
	2.49 (2.43)	2.46	3.32 (3.21) × 2	3.30 × 2
	2.52 (2.59)	2.55	3.32 (3.18) × 2	3.36 × 2
	2.66 (2.68)	2.60	3.33 (3.24) × 2	3.39 × 2
	2.71 (2.81)	2.72		
	2.73 (2.76)	2.82		
	2.74 (2.68)	3.04		
	Ae–H			
Ae1-H	2.06–2.36 (2.07–2.33)	2.04–2.77	2.94–3.31 (2.89–3.20)	2.87–3.17
Ae2-H	2.14–2.88 (2.20–2.77)	2.11–3.32	2.79–2.99 (2.71–2.94)	2.78–3.02
Ae3-H	2.01–2.24 (1.97–2.30)	1.99–2.43		

^a Experimental values are given in parantheses. Distance ranges Ae–H refer to those within the coordination polyhedra shown in Figure 1.

comparison of Ba_2PdH_4 and Mg_2NiH_4 with hypothetical Mg_2PdH_4 and Ba_2NiH_4 is very instructive.

Mg_2PdH_4 and Ba_2NiH_4 . The DOS of Ba_2NiH_4 (Figure 5c) is very similar to that of Ba_2PdH_4 (cf. Figure 5a). The only difference is that in the former the bonding a_1 and t_2 based bands are resolved. Because both systems are isostructural (β - K_2SO_4 type) and have the same kind of counterions, we now can directly compare bonding in the tetrahedral complexes $T^0H_4^{4-}$. Importantly, it is unambiguously corroborated that Ni–H interactions are considerably smaller than Pd–H ones. This is first manifested in the DOS of Ba_2NiH_4 by the smaller splitting between e and $2t_2$ states and the higher lying bonding t_2 states compared to those of Ba_2PdH_4 . Second, the low contribution of Ni-d states to the bonding ($a_1 + t_2$) part of the DOS compared to the Pd-d ones (Table 4) completes this picture. We may simply attribute the differences in bonding between Ni and Pd hydrido complexes to the well-known fact that the 4d orbitals of Pd are more diffuse than the Ni-3d ones and thus make stronger orbital interaction to the H ligands.³⁵ Most interesting, the equilibrium Ni–H distances in Ba_2NiH_4 are about

0.1 Å longer than in Mg_2NiH_4 (cf. Table 5), and the value of 1.64 Å coincides with that obtained from molecular calculations of a single tetrahedral NiH_4^{4-} complex.³⁶ Thus, the short Ni–H distances in Mg_2NiH_4 are a consequence of the Mg^{2+} counterion matrix. The requirement of Mg^{2+} for small H coordination numbers acts as internal pressure on the compound, compressing the $Ni^0H_4^{4-}$ entity and decreasing intertetrahedral distances. This fact is also seen in Mg_2PdH_4 where the Pd–H distances are decreased by about 0.08 Å compared to those of Ba_2PdH_4 , and further, the shortest intertetrahedral distances become smaller than the intratetrahedral ones. The DOSs of Mg_2NiH_4 and Mg_2PdH_4 (Figure 5b,d) are similar. However, again, Pd–H interactions are stronger than Ni–H ones (cf. Table 4).

In conclusion, we observe quite different bonding situations in the ternary hydrides Ba_2PdH_4 and Mg_2NiH_4 , which both contain, formally, discrete $T^0H_4^{4-}$ complexes. The former can electronically be described as a complex transition metal hydride where the molecular states of the complex entity in the DOS of the solid state compound are clearly recognizable. In contrast, Mg_2NiH_4 behaves electronically rather as a hybrid, that is, partly as an ionic hydride ($Mg^{2+}(H^-)_2$) and partly as hydrido complex compound ($(Mg^{2+})_2Ni^0H_4^{4-}$), to meet the coordination requirement of the small and polarizing counterions Mg^{2+} . The peculiarity of Mg as Ae component in hydrides is already manifested in the binary, ionic, compound MgH_2 . In Figure 6, we compare the DOS of rutile MgH_2 with $BaCl_2$ -type BaH_2 . For MgH_2 , the H based valence band has a dispersion of more than 6 eV, whereas in BaH_2 it is confined to a range of 3 eV. Again, this dispersion basically originates from closed-shell interaction between the hydride ions and to a minor extent from the Ae–H interaction. In rutile MgH_2 , Mg^{2+} is coordinated by six H^- , and H^- , by three Mg^{2+} ions, and these small coordination numbers yield short H–H distances of 2.49 Å (calculated) and Mg–H distances of 1.95 Å.

4. Conclusions

Bonding and stability of monoclinic Mg_2NiH_4 and orthorhombic Ba_2PdH_4 were investigated by ab initio density functional calculations using pseudopotentials and a plane wave basis set. The calculational method reproduced very well the correct ground state structures, the experimental structural parameters, and available experimental data of physical properties of these hydrides. Especially, the excellent agreement of the experimentally determined atomic position parameters with the computationally modeled ones underlines the possibility to use modern calculational methods for the refinement of hydrogen positions in hydrides in those cases where neutron diffraction experiments cannot be performed.³⁷

The semiconducting compounds Mg_2NiH_4 and Ba_2PdH_4 belong to the family of complex transition metal hydrides. Both structures contain discrete tetrahedral 18 electron complexes $T^0H_4^{4-}$. However, the bonding situation turns out

(35) Huheey, J. E.; Keiter, E. A.; Keiter, R. L. *Inorganic Chemistry: Principles of Structure and Reactivity*, 4th ed.; Harper Collins College Publishers: New York, 1993.

(36) Lindberg, P.; Noréus, D.; Blomberg, M. R. A.; Siegbahn, P. E. M. *J. Chem. Phys.* **1986**, *85*, 4530.

(37) Milman, V.; Winkler, B. Z. *Kristallogr.* **2001**, *216*, 99.

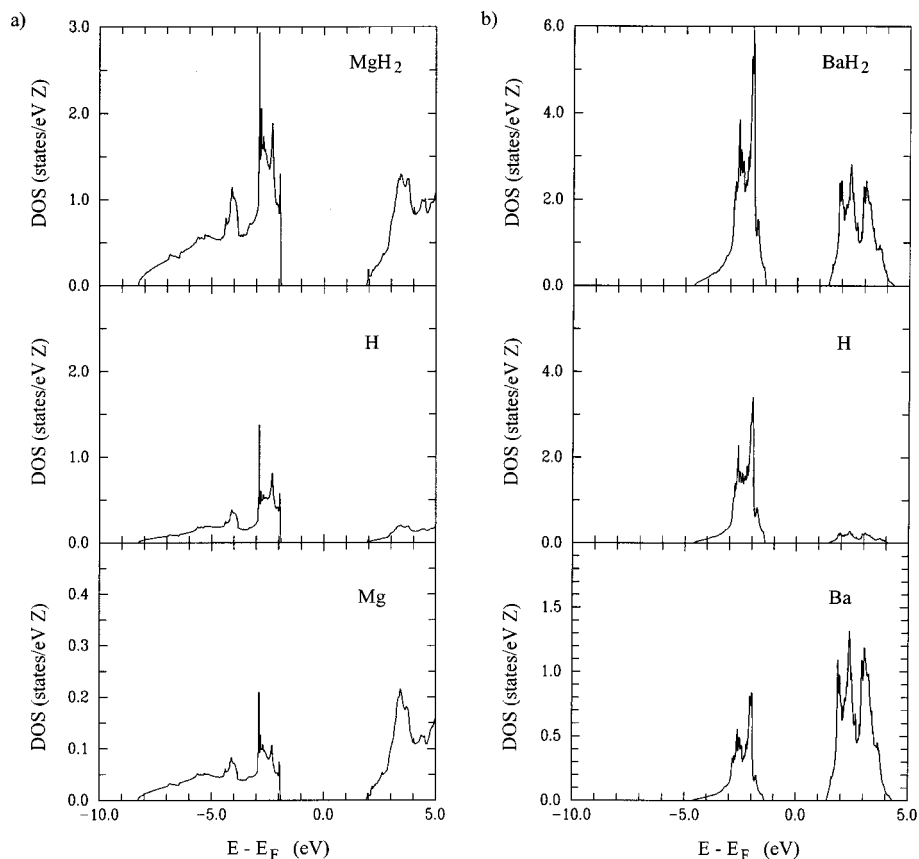


Figure 6. Total DOS and partial DOS of the sites H and Ae of the binary systems MgH_2 (a) and BaH_2 (b) calculated at the theoretical equilibrium volume of the respective ground-state structure. The Fermi level, E_F , is set to zero.

to be quite different in the two systems. For Ba_2PdH_4 , the DOS clearly mirrors the molecular states of the complex PdH_4^{4-} . Because Pd-p (and Ni-p) orbitals are basically bonding inactive, Pd–H antibonding states have to be occupied in the 18 electron complex leading to a weakly bonded species PdH_4^{4-} . This unfavorable situation is improved by stabilizing interactions of the surrounding counterion matrix in the solid state. The admixture of empty Ba^{2+} states to the occupied bands partly releases antibonding states above the Fermi level. Compared to Ba_2PdH_4 for Mg_2NiH_4 , we find weak T–H interactions and, because of the small size and high polarizing power of Mg^{2+} , strong Ae–H interactions. The clear relation between molecular states of TH_4^{4-} and DOS of the solid-state compound is lost. Mg_2NiH_4 and $CaMgNiH_4$ (with a different structure) are the only known compounds with Ni hydrido complexes. Apparently, because of the weak Ni–H interactions, polarizing counterions are needed in order to obtain Ni hydrido complexes in the solid state. This may also explain why no Ni hydrido complexes have been found with alkali metal counterions.

Finally, Mg_2NiH_4 is considered to be a promising hydrogen storage material with a 3–4 times better weight efficiency than commercially used hydrides.¹ The utility of Mg_2NiH_4 is based on the fortuitous formation of the alloy Mg_2Ni in the desorption reaction $Mg_2NiH_4 \rightarrow Mg_2Ni + 2H_2$ which has a considerably lower enthalpy compared to the decomposition into the elements (cf. Figure 3). However, the desorption temperature of Mg_2NiH_4 is still too high for most

technical applications. The desirable lowering of the thermal stability of this material can either be achieved by a destabilization of the hydride or/and a stabilization of the alloy Mg_2Ni . One possibility might be a partial chemical substitution of Mg by a trivalent metal (e.g. by Al). Because $Ni^0H_4^{4-}$ represents an 18 electron complex, this doping would introduce defects into the counterion matrix, i.e., $Mg_{2-1.5x}Al_x \square_{x/2}NiH_4$ (\square = vacancy), and could destabilize the hydride. It is, for example, known that the lattice amorphization of Mg_2NiH_4 by ball-milling strongly influences the desorption reaction.³⁸ Hirata indeed observed a fairly substantial destabilization in slightly Al-doped Mg_2NiH_4 ($x_{Al} \approx 0.08$) already almost 20 years ago.³⁹ However, no systematic investigation concerning the homogeneity range and the structural consequences of the doping was performed. Prerequisite for success of doping experiments is that the trivalent metal is also incorporated in the alloy Mg_2Ni . It is known that intermetallic compounds with the Mg_2Ni structure type have a homogeneity range with respect to the electron concentration,⁴⁰ and there are many examples of ternary intermetallic compounds with mixed occupied (Mg/Al) positions.⁴¹ Thus,

(38) Zaluska, A.; Zaluski, L.; Ström-Olsen, J. O. *J. Alloys Compd.* **1999**, 289, 197.

(39) Hirata, T.; Matsumoto, T.; Amano, M.; Sasaki, Y. *J. Less-Common Met.* **1983**, 89, 85. Hirata, T. *Int. J. Hydrogen Energy* **1984**, 9, 855.

(40) Häussermann, U.; Simak, S. I.; Abrikosov, I. A.; Johansson, B.; Lidin, S. *J. Am. Chem. Soc.* **1998**, 120, 10136.

(41) Villars, P.; Calvert, L. D. *Pearsons Handbook of Crystallographic Data for Intermetallic Compounds*, 2nd ed.; ASM International: Materials Park, OH, 1991.

Al might be a very promising candidate for a more elaborate and systematic optimization of the hydrogen storage properties by varying the composition of quaternary $\text{Mg}_{2-x}\text{Al}_x\text{NiH}_4$. Additionally, the introduction of defects may reveal interesting structural properties for this system.

Acknowledgment. This work was supported by the Swedish National Science Research Council (NFR) and the Foundation for Strategic Environmental Research (MISTRA).

Note Added in Proof. Recently, Myers et al. reported calculated thermodynamic, electronic, and optical properties of monoclinic Mg_2NiH_4 .⁴² The authors used a plane wave basis together with normconserving pseudopotentials. (We

employed a plane wave basis and ultrasoft Vanderbilt-type pseudopotentials.) Their results concerning relaxed atomic position parameters and density of states of monoclinic Mg_2NiH_4 correspond virtually to our findings. However, the calculated enthalpy of the hydrogenation reaction $\text{Mg}_2\text{Ni} + 2\text{H}_2 \rightarrow \text{Mg}_2\text{NiH}_4$ was -2.06 eV/Z. This is rather different from our value of -1.30 eV/Z. We attribute this discrepancy to the fact that Myers et al. did not perform an optimization of the lattice parameters of the alloy Mg_2Ni but used the experimental values.

IC0201046

(42) Myers, W. R.; Wang, L.-W.; Richardson, T. J.; Rubin, M. D. *J. Appl. Phys.* **2002**, *91*, 4879.